RECENT DEVELOPMENTS IN SPARSE HYPERSPECTRAL UNMIXING

Marian-Daniel Iordache, Antonio Plaza

Department of Computer Science
University of Extremadura
E-10071 Cáceres, Spain

José Bioucas-Dias

Instituto Superior Técnico
Instituto de Telecomunicações
Av. Rovisco Pais, 1049-001 Lisboa, Portugal

ABSTRACT

This paper explores the applicability of new sparse algorithms to perform spectral unmixing of hyperspectral images using available spectral libraries instead of resorting to well-known endmember extraction techniques widely available in the literature. Our main assumption is that it is unlikely to find pure pixels in real hyperspectral images due to available spatial resolution and mixing phenomena happening at different scales. The algorithms analyzed in our study rely on different principles, and their performance is quantitatively assessed using both simulated and real hyperspectral data sets. The experimental validation of sparse techniques conducted in this work indicates promising results of this new approach to attack the spectral unmixing problem in remotely sensed hyperspectral images.

***Index Terms*—** Hyperspectral unmixing, sparse regression, convex optimization, spectral libraries.

1. INTRODUCTION

The wealth of spectral information available from advanced hyperspectral imaging instruments currently in operation has opened new perspectives in many application domains [1]. Exploring the information contained in hyperspectral data sets is a challenging problem, not only from the viewpoint of inferring information at sub-pixel levels, but also because of the need to develop robust and fast algorithms. For instance, the *spectral signature* of a pixel in a hyperspectral image is obtained from the reflectance values of that material for a specific range of wavelengths which can be in the order of hundreds [2]. If the spatial resolution of the sensor is not high enough to separate different materials, these can jointly occupy a single pixel. As a result, most of the pixels of a hyperspectral image are mixed in nature [3].

To deal with the mixture problem, linear spectral mixture analysis techniques first identify a collection of spectrally pure constituent spectra, called *endmembers* in the literature [4], and then express the measured spectrum of each mixed pixel as a linear combination of endmembers weighted by fractions or abundances that indicate the proportion of each endmember present in the pixel. It should be noted that the linear mixture model assumes minimal secondary reflections and/or multiple scattering effects in the data collection procedure, and hence the measured spectra can be expressed as a linear combination of the spectral signatures of materials present in the mixed pixel [3]. Quite opposite, the nonlinear mixture model assumes that the endmembers form an intimate mixture inside the respective pixel, so that incident radiation interacts with more than one component and is affected by multiple scattering effects [5]. Nonlinear unmixing generally requires prior knowledge about object geometry and physical properties of the observed objects. In this work we will focus exclusively on the linear mixture model due to its computational tractability and flexibility in different applications.

In this work, we adopt a novel semi-supervised approach to linear spectral unmixing which relies on the increasing availability of spectral libraries of materials measured on the ground, for instance, using advanced field spectroradiometers. Our main assumption is that mixed pixels can be expressed in the form of linear combinations of a number of pure spectral signatures known in advance and available in a library. When the unmixing problem is approached using spectral libraries, the abundance estimation process no longer depends on the availability of pure spectral signatures in the input data nor on the capacity of a certain endmember extraction algorithm to identify such pure signatures. Quite opposite, the procedure is reduced to finding the optimal subset of signatures in the library that can best model each mixed pixel in the scene. Despite the appeal of this semi-supervised approach to spectral unmixing, it is subjected to several potential drawbacks:

1. One risk in using library of endmembers is that these spectra are rarely acquired under the same conditions as the airborne data. Image endmembers have the advantage of being collected at the same scale as the data and can, thus, be more easily associated with features on the scene. However, such image endmembers may not always be present in the input data. In this work, we rely on the use of advanced atmospheric correction algorithms which convert the input hyperspectral data from at-sensor radiance to reflectance units.

2. Most importantly, if a large spectral library is used, it

is likely that the number of spectral endmembers contributing to a mixed pixel, will be generally very small compared with the total number of spectra in the library. In this case, the abundance vector is sparse and its estimation can benefit from the use of sparse regression techniques based on sparsity-inducing regularizers.

3. Finally, since the number of endmembers participating in a mixed pixel is usually very small compared with the (ever-growing) dimensionality –and availability– of spectral libraries, techniques able to perform sparse regression and convex optimization in computationally efficient fashion are also required.

In this paper, we specifically address the problem of sparsity when unmixing hyperspectral data sets using spectral libraries, and further provide a quantitative and comparative assessment of several available and new convex optimization and sparse regression algorithms which can be used for this purpose.

2. THE SPARSE UNMIXING APPROACH

A semi-supervised approach is proposed to look for the endmembers in a spectral library containing spectra of many materials, with only a few of them present in a pixel. This means that the vector of fractional abundances is *sparse*. This is the central point of sparse unmixing techniques: they enforce the sparsity of the solution explicitly, as opposed to non-sparse techniques which aim at finding the correct set of endmembers from the spectral library but do not enforce sparseness explicitly. Examples of non-sparse techniques can be found in [4].

In this work, two different formulations of the sparse unmixing problem are presented and discussed. Specifically, we show some of the characteristics of the unmixing problem that limit the performance of these techniques and their applicability in simulated and real environments. The sparse techniques will be exemplified using the following algorithms: Constrained Sparse Unmixing algorithm via variable Splitting and Augmented Lagrangian - CSUnSAL, Sparse Unmixing algorithm via variable Splitting and Augmented Lagrangian - SUnSAL, and Two-Step Iterative Shrinking/Thresholding algorithm - TwIST [6]. CSUnSAL corresponds to the first formulation of the sparse unmixing problem, while TwIST and SUnSAL correspond to the second one. The two formulations are further explained below. CSUnSAL and SUnSAL are, respectively, variants of the algorithms presented in [7] and [8, 9], tailored to hyperspectral data. In all cases, we rely on a linear mixing model, expressed for one pixel in compact notation as follows:

$$r = Mx + n \tag{1}$$

Considering that the sensor acquires the information in L bands and there are q endmembers present in the pixel, $\mathbf{r}$ is an L-by-1 column vector representing the measured spectrum of the pixel, M is an L-by-q matrix called *the mixing matrix* (the spectral signatures of the endmembers), x is a q-by-1 column-vector (the respective fractional abundances of the endmembers) and n is an L-by-1 column-vector collecting the errors affecting the measurements. If the spectral library S contains p signatures (so it is an L-by-p matrix), the model in Eq. (1) can be reformulated as follows:

$$r = Sf + n \tag{2}$$

In Eq. (2), we changed the notation of the vector collecting the fractional abundances, as the new vector f has p components, of which only q are non-zero. In a practical scene, it is true that $q << p$ and, by consequence, f is a sparse vector. There are different techniques commonly used in order to impose the sparsity of the solution in the hyperspectral unmixing problem. The problem is initially formulated as an optimization problem as follows:

$$\min_{f} \|f\|_0 \;\; \text{subject to} \;\; \mathrm{S\,f} = R \tag{3}$$

where $||f||_0$ denotes the l_0 norm of f, which simply counts the non-zero components in f. The optimization problem shown in Eq. (3) offers the possibility to compute the exact solution of the system if the observation is not affected by errors. Unfortunately, it represents a (NP-hard [10]) non-convex problem, which is very difficult to solve, and there are errors affecting the observed spectrum due to the electronic noise and to the speed of the sensor flying at high altitudes. As it was shown in [11], under certain conditions the l_0 norm can be replaced by the l_1 norm. We can implement now a relaxation of the problem stated in Eq. (3) as follows:

$$\min_{f} \|f\|_1 \;\; \text{subject to} \;\; \|Sf - R\|_2 \leq \delta. \tag{4}$$

The optimization problem in Eq. (4) is a convex, which is easier to solve. This is the first formulation of the sparse unmixing problem that we take into account in this paper and it is solved using the CSUnSAL algorithm. The same algorithm will be used to solve the same problem, but taking into account the abundance non-negativity (ANC) constraint:

$$\min_{f} \|f\|_1 \quad \text{subject to} \quad \|Sf - R\|_2 \leq \delta, \quad f \geq 0. \tag{5}$$

The second formulation of the sparse unmixing problem is expressed under the form of an $l_2 - l_1$ norm minimization problem. This form results from Eq. (4) by bringing the constraint inside the objective function:

$$\min_{f} \frac{1}{2}\|Sf - R\|_2^2 + \lambda\|f\|_1 \tag{6}$$

where the first term of the objective function measures the lack of fitness of a candidate to the solution and the second terms measures the lack of sparsity. The scalar parameter λ has the role of weighting the two terms. This problem is solved, in this paper, by TwIST algorithm. SUnSAL is used to solve the same objective function 6, in which we enforce the ANC constraint:

$$\min_f \frac{1}{2}\|Sf - R\|_2^2 + \lambda\|f\|_1 \quad \text{subject to} \quad f \geq 0. \qquad (7)$$

3. EXPERIMENTAL RESULTS

3.1. Simulated data

In order to evaluate the performances of sparse unmixing algorithms, in this subsection we describe the results obtained after applying them to simulated hyperspectral data. The spectral library S used in experiments was generated using our own spectral library generator tool, which allows an user to create a spectral library starting from the ASTER library[1], a compilation of over 2400 spectra of natural and man made materials. Specifically, we generated a library which contains 230 members, each of which has the reflectance values measured for 224 spectral bands distributed uniformly in the interval 3-10μm. Using the library S, four hyperspectral data sets were generated, each of them containing 200 samples.

The term n in (1), in real applications, is highly correlated because it is mostly due to modeling errors and the spectra are of of low-pass type with respect to the wavelength. Accordingly, we considered, in experiments, that term n results from low- pass filtering independent and identically distributed (iid) Gaussian noise. We have used a normalized cut-of frequency of $10\pi/L$. The amplitude of the noise was chosen such that the signal-to-noise-ratio (SNR $\equiv ||Sf||^2/||n||^2$) takes values: ∞ (noiseless observation), 35dB, 30dB, 25dB and 20dB.

We consider four data sets corresponding to sparsities of the fractional abundances x (i.e., the number of non-zero components of x) of 5, 10, 15 and 20 members, respectively. We stress that in hyperspectral applications, the sparsity of fractional abundances is small, most likely less of equal than 5.

Before describing our obtained results, it is important to emphasize that the problem that we are solving is difficult, first of all, because of the characteristics of the considered spectral library. Specifically, it has been shown that the quality of the reconstruction of a spectral signature using the linear mixture model (which can be measured, e.g., using the reconstruction signal-to-noise ratio RSNR $\equiv E[f^2]/(E[f - \widehat{f}])$, where $E[\cdot]$ stands for mean value and $\widehat{f}$ is the computed factional abundances) decreases when the mutual coherence of the library, $\mu(S)$, approaches 1 [11]. A simple test shows that, in our case, the mutual coherence of the considered library is $\mu(S) \approx 1$; this characteristic of S is a good indicator of the high difficulty of this problem. The fact hyperspectral fractional abundances are very sparse attenuates, however, the hardness of the sparse regression problem at hand.

Table 1 shows the RSNR obtained for different sparse unmixing methods with libraries using different number of members (the parameter settings used to arrive to these results will be detailed at the final version of the paper), measured in dBs, i.e RSNR(dB) $\equiv 10\log_{10}$(RSNR).

From Table 1, it can be observed that, for noiseless data, all the algorithms have good performances, CSUNSAL being the most efficient. As expected, the accuracy of the results decreases at the same with the decreasing SNR, for all the methods. For the given problem, CSUnSAL returns the most accurate results in all the situations, but, from the experience of the authors, it can not be claimed to be "better" than SUnSAL in general, as SUnSAL attains comparable (and sometimes better) performances as CSUnSAL when the noise affecting the measurements is white. CSUNSAL is, also, the method which has the most abrupt degradation of the relative error when the level of noise increases. SUNsAL attains better accuracies of the results than TwIST when the level of the noise is not very high, but TwIST performs better than SUnSAL in the later case, although, in its case, the ANC constraint is not enforced. All the methods loose accuracy when the number of endmembers present in the mixture increases, as expected. However, at least in the absence of noise, we still obtain good sparse regressions for fractional abundances with up to 20 non-zero components, what is more than enough in most hyperspectral applications.

Unmixing results obtained in a real scene using the sparse approach in the context of predefined spectral library are shown in the following subsection.

3.2. Experimental results with real data

This subsection exemplifies the practical applicability of the sparse unmixing algorithms (represented here by SUnSAL (ANC)), for real data. The scene used in experiments is the well-known AVIRIS Cuprite data set, available online in reflectance units[2]. The portion used in experiments corresponds to a 350×350-pixel subset, comprising 224 spectral bands between 0.4 and 2.5 m, with nominal spectral resolution of 10 nm. Prior to the analysis, bands 1–2, 105–115, 150–170, and 223–224 were removed due to water absorption and low SNR in those bands, leaving a total of 188 spectral bands.

Fig. 1 shows abundance maps obtained for several materials present in the scene using a hyperspectral library containing 498 pure signatures of minerals selected from the USGS splib06[3] library, released in September 2007. Different comparisons to reference maps available from USGS reveal that

[1] Available online: http://speclib.jpl.nasa.gov

[2] http://aviris.jpl.nasa.gov/html/aviris.freedata.html

[3] http://speclab.cr.usgs.gov/spectral.lib06

Table 1. RSNR obtained by different sparse unmixing methods with simulated hyperspectral mixtures.

Members	SNR	CSUnSAL (unconstrained)	CSUnSAL (ANC)	TwIST (unconstrained)	SUnSAL (ANC)
5	∞	26.69	30.91	7.64	9.97
	35dB	17.05	16.23	7.54	8.56
	30dB	13.75	11.82	6.49	6.70
	25dB	7.78	7.39	6.00	4.66
	20dB	-0.36	2.27	4.64	1.00
10	∞	22.70	27.08	5.78	6.95
	35dB	16.70	14.68	5.56	5.92
	30dB	11.29	9.42	5.20	4.80
	25dB	5.35	5.13	5.04	2.89
	20dB	-2.45	0.05	3.39	-0.63
15	∞	20.68	24.45	4.82	5.57
	35dB	14.40	13.03	4.4229	5.0721
	30dB	10.40	8.70	4.14	4.31
	25dB	4.23	4.09	3.58	2.12
	20dB	-3.70	-1.34	2.56	-1.89
20	∞	16.92	18.80	4.16	4.62
	35dB	12.83	11.54	3.49	3.79
	30dB	8.41	6.88	3.34	2.99
	25dB	3.89	3.37	2.81	1.79
	20dB	-3.74	-1.84	1.69	-2.286

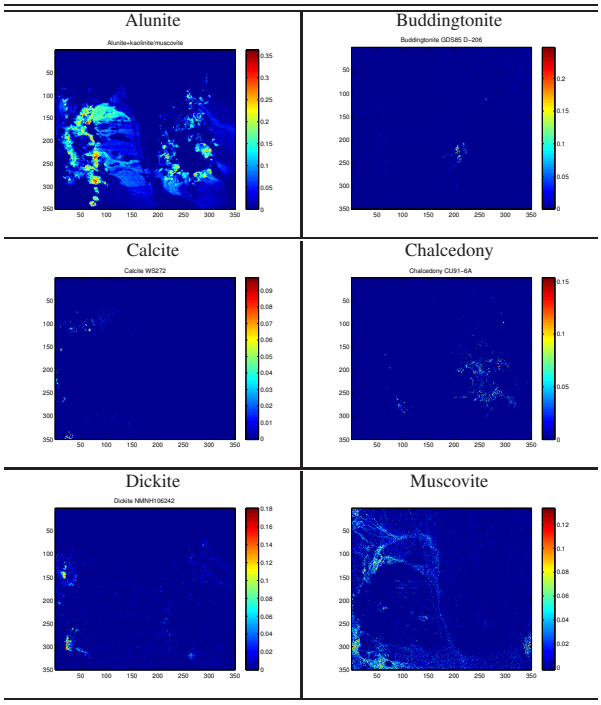

Fig. 1. Abundance maps obtained by SUnSAL (ANC) for the Cuprite scene.

the obtained abundance maps provide accurate estimates of mineral distributions in the AVIRIS Cuprite mining district.

4. ACKNOWLEDGMENT

This work has been supported by the European Community's Marie Curie Research Training Networks Programme under contract MRTN-CT-2006-035927, Hyper-spectral Imaging Network (HYPER-I-NET).

5. REFERENCES

[1] C.-I Chang, *Hyperspectral Imaging: Techniques for Spectral Detection and Classification*, Kluwer Academic/Plenum Publishers: New York, 2003.

[2] R. O. Green, M. L. Eastwood, C. M. Sarture, T. G. Chrien, M. Aronsson, B. J. Chippendale, J. A. Faust, B. E. Pavri, C. J. Chovit, M. Solis, et al., "Imaging spectroscopy and the airborne visible/infrared imaging spectrometer (AVIRIS)," *Remote Sensing of Environment*, vol. 65, no. 3, pp. 227–248, 1998.

[3] J. B. Adams, M. O. Smith, and P. E. Johnson, "Spectral mixture modeling: a new analysis of rock and soil types at the Viking Lander 1 site," *Journal of Geophysical Research*, vol. 91, pp. 8098–8112, 1986.

[4] A. Plaza, P. Martinez, R. Perez, and J. Plaza, "A quantitative and comparative analysis of endmember extraction algorithms from hyperspectral data," *IEEE Transactions on Geoscience and Remote Sensing*, vol. 42, no. 3, pp. 650–663, 2004.

[5] N. Keshava and J. F. Mustard, "Spectral unmixing," *IEEE Signal Processing Magazine*, vol. 19, no. 1, pp. 44–57, 2002.

[6] J. M. Bioucas-Dias and M. A. T. Figueiredo, "A new twist: Two-step iterative shrinkage/thresholding algorithms for image restoration," *IEEE Transactions on Signal Processing*, vol. 16, pp. 2992–3004, 2007.

[7] M. Afonso, J. Bioucas-Dias, and M. Figueredo, "A fast algorithm for the constrained formulation of compressive image reconstruction and other linear inverse problems," in *submitted to the 2010 IEEE International Conference on Acoustics, Speech and Signal Processing*, 2010.

[8] M. Afonso, J. Bioucas-Dias, and M. Figueredo, "Fast image recovery using variable splitting and constrained optimization," *submitted to the IEEE Transactions on Image Processing, 2009*, 2009.

[9] J. Bioucas-Dias, "A variable splitting augmented lagrangian approach to linear spectral unmixing," *First IEEE GRSS Workshop on Hyperspectral Image and Signal Processing - WHISPERS'2009, Grenoble, France*, 2009.

[10] B. Natarajan, "Sparse approximate solutions to linear systems," *SIAM Journal on Computing*, vol. 24, pp. 227, 1995.

[11] A. M. Bruckstein, D. L. Donoho, and M. Elad, "From sparse solutions of systems of equations to sparse modeling of signals and images," *SIAM Review*, vol. 51, pp. 34–81, 2009.